PHYSICAL REVIEW B VOLUME 40, NUMBER 15 15 NOVEMBER 1989-II

Isolated arsenic-antisite defect in GaAs and the properties of *EL*2

Jaroslaw Dabrowski* and Matthias Scheffler

Fritz-Haber-Institut der Max-Planck-Gesellschaft, Faradayweg 4-6, D-1000 Berlin 33, West Germany

(Received 12 May 1989)

We report parameter-free, self-consistent calculations of the electronic structures, total energies, and forces of the $\mathrm{As_{Ga}}$ antisite, of an As-interstitial–Ga-vacancy defect pair, and of various configurations between these limits. The corresponding total-energy surface exhibits an interesting metastability. The results are discussed with respect to photoquenching, thermal stability, optical, electronic, and magnetic properties of *EL*2. This comparison shows that the behavior of *EL*2 may be understood in terms of the isolated arsenic antisite, which exhibits via the mentioned metastability ($\mathrm{As_{Ga}} \rightleftharpoons V_{\mathrm{Ga}}\mathrm{As}_i$) and the dissociation and/or association ($\mathrm{As_{Ga}} \rightleftharpoons V_{\mathrm{Ga}} + \mathrm{As}_i$) a variety of different properties. It is pointed out that this new mechanism of metastability may be significant for other point defects in semiconductors as well.

I. INTRODUCTION

The *EL*2 defect is the dominant deep donor in undoped gallium arsenic crystals, which are grown under As-rich conditions. An understanding of this defect is important in view of the basic task of understanding the electronic, electric, optical, and magnetic properties of clean, real crystals. A particular challenge is the understanding of metastabilities, and in this respect *EL*2 exhibits an interesting behavior: At low temperatures, illumination with white light (precisely $\hbar\omega \geq 1.18$ eV) makes the deep *EL*2 level disappear (see Fig. 1), and then the defect could no longer be detected by any experimental method.[1,2] Heating the sample to $T > 140$ K brings the defect and its deep level back in full concentration. Further details of this metastability are discussed below. There is also significant technological interest in the *EL*2 defect, because owing to its high concentration *EL*2 provides enough electrons to compensate intrinsic and residual-impurity acceptors and pins the Fermi level in the middle of the forbidden gap.

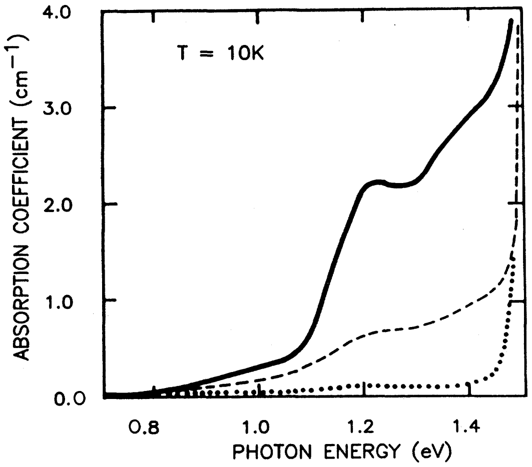

FIG. 1. Experimental result of the photoquenching of *EL*2 at low temperature (after Ref. 1). The solid curve shows the absorption in the dark, which starts at 0.75 eV and has a bump at 1.18 eV. After illumination with white light for 1 min, the absorption spectrum is changed to the dashed curve. After illumination for 10 min it is changed to the dotted curve. The *EL*2 absorption can be completely bleached away (at $T < 140$ K), and then the defect was not longer found by any experimental method.

Optically or thermally inducible defect metastabilities have been well known for years.[3-6] The best understood metastable centers are iron-acceptor pairs.[3] In fact, all metastable defects identified so far are complexes, where the metastability is understood in terms of a rearrangement of one of the constituents. It therefore appears plausible that also most of the microscopic models for *EL*2, which are discussed in the literature, are complexes. Because *EL*2 is accepted as not being impurity related,[2,7] these models are built from native defects. The most often discussed models for *EL*2 are aggregates of several $\mathrm{As_{Ga}}$ defects,[8,9] complexes of $\mathrm{As_{Ga}}$ with vacancies,[10,11] and the distant $\mathrm{As_{Ga}}$-As_i pair.[12-21] Here, $\mathrm{As_{Ga}}$ stands for an As antisite, i.e., an As atom occupying what is normally a Ga site (see Fig. 2), and As_i stands for an As interstitial.

In the last few years the distant $\mathrm{As_{Ga}}$-As_i pair, in particular, has attracted attention. von Bardeleben *et al.*[12,13] proposed the pair model on the basis of sys-

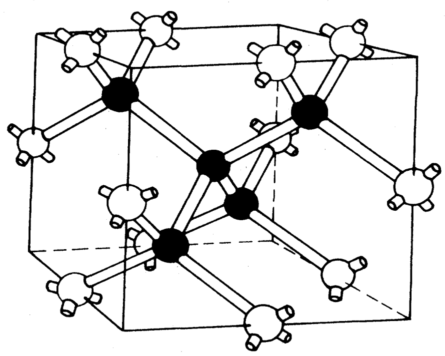

FIG. 2. Atomic geometry of the isolated arsenic antisite. Solid circles are As atoms, open circles are Ga atoms.

tematic thermal deep-level transient spectroscopy (DLTS) studies, which strongly indicated the existence of an As_i in the $EL2$ formation process. This $\mathrm{As}_{\mathrm{Ga}}$-$\mathrm{As}_i$-pair model was strengthened by electron-nuclear double-resonance (ENDOR) studies by Meyer *et al.*[15-17] who concluded that the ENDOR data are due to a distant $\mathrm{As}_{\mathrm{Ga}}$-$\mathrm{As}_i$ pair, that the defect symmetry is C_{3v}, and that the separation between the $\mathrm{As}_{\mathrm{Ga}}$ and As_i was 4.88 Å. Theoretical work by Baraff *et al.*[19,20] and by Caldas and Fazzio[21] gave support for the $\mathrm{As}_{\mathrm{Ga}}$-$\mathrm{As}_i$-pair model, and Delerue *et al.*[18] explained the pair's metastable geometry in terms of a displaced As_i. All these theoretical studies were based on semiempirical, parametrized calculations.

Based on self-consistent total-energy calculations,[22-24] we recently questioned some details of the ENDOR analysis. In particular, we found that the 4.88-Å separation does not correspond to a stable or metastable geometry. In fact, our calculations indicated that a distant pair is practically unbound. This makes it an unlikely candidate for the dominant defect in GaAs. Last but not least, we noted that the pair should have a shallow level close to the conduction band, which seems to be in conflict with what is known to date about the $EL2$ center. We therefore speculated[23,24,3] that the ENDOR (Refs. 15-17) and EPR (Refs. 25-27) data are due to a different complex, $\mathrm{As}_{\mathrm{Ga}}$-$X$, where X stands for an acceptor, not just a distant As interstitial. We also emphasized[23,24] that EPR and ENDOR probe a different charge state than that studied by optical absorption.[1]

Direct investigations of the symmetry of the $EL2$ defect, when in the charge state, which shows the characteristic $EL2$ absorption and the interesting metastability, are absorption studies under uniaxial pressure. These experiments, by Kaminska *et al.*,[28-30] give no indication of a complex defect, but show tetrahedral symmetry. Recently, these measurements were repeated by other groups.[31,32] Up to now, the suggestion of Kaminska *et al.*[28-30] that $EL2$ has tetrahedral symmetry and that it is identical to the isolated $\mathrm{As}_{\mathrm{Ga}}$ antisite was not generally accepted (see, for example, Refs. 33-35), because a simple Huang-Rhys picture, together with the assumption that the defect couples only to a single-phonon mode, was inconsistent with the experimental line shape,[36] and it was questioned that "optical absorption at the isolated antisite can produce the observed metastability."[19] Bachelet and Scheffler[37,38] had, however, already suggested such a mechanism five years ago. A careful calculation of this suggested process was not possible at that time, but became possible recently. These parameter-free calculations of the optically excited $\mathrm{As}_{\mathrm{Ga}}$ antisite are described below (also see Ref. 22). They confirm and specify the prediction of Bachelet and Scheffler.[37,38]

This short discussion shows the difficulty and active controversy about the $EL2$ center, of which even the most basic property, namely its symmetry, is not generally agreed on. Much of the controversy over the $EL2$ defect is due to the fact that the experimental literature on $EL2$ is enormously voluminous and many experimental results seem to contradict others. This is partly due to the fact that an unambiguous distinction of properties which are directly due to $EL2$ from properties of other defects, which also change when $EL2$ is studied, is difficult. Furthermore, for a discussion of $EL2$ often only a certain class of experiments is considered in the discussion. We feel that it is important to take different experimental studies into account, which cover (1) photo quenching, (2) thermal stability, (3) optical, (4) electron, and (5) magnetic properties.

In Ref. 22 (also see Sec. II) we therefore compiled a list of what we call the (at this time) "experimentally established properties of $EL2$." We also performed calculations for all intrinsic point defects in GaAs and for the distant $\mathrm{As}_{\mathrm{Ga}}$-$\mathrm{As}_i$ pair.[22-24] In the present paper we give a detailed description of our quantum-mechanical calculations of the $\mathrm{As}_{\mathrm{Ga}}$ antisite in GaAs in its ground state and in an optically excited state. We show how the latter drives the originally fourfold-coordinated arsenic defect atom from the $\mathrm{As}_{\mathrm{Ga}}$ antisite configuration to a different (threefold-coordinated) configuration, namely a $V_{\mathrm{Ga}}\mathrm{As}_i$ defect pair. This study explains a basic mechanism of optical quenching and thermal recovery of a simple point defect. Based on our list of $EL2$ properties and on our theoretical results, we identify the basic mechanism of the $EL2$ metastability with that of the $\mathrm{As}_{\mathrm{Ga}} \leftrightarrows V_{\mathrm{Ga}}\mathrm{As}_i$ structural transition.

The remaining paper is organized as follows. In Sec. II we summarize what appears to be the experimentally established properties of $EL2$. Then, in Sec. III we describe the theoretical method. In Sec. IV we present our calculated results for the ground state of the $\mathrm{As}_{\mathrm{Ga}}$ antisite, its optically excited state, and its transition to a metastable configuration, namely the $V_{\mathrm{Ga}}\mathrm{As}_i$ defect pair. Then in Sec. V we compare our theory of Sec. IV with the experimental properties of the $EL2$ defect. In Sec. VI we summarize our conclusions.

II. THE *EL*2 DEFECT IN GALLIUM ARSENIDE

A careful discussion of the $EL2$ center requires us to take a variety of different properties into account. We therefore start with a list of the most important "experimentally established properties of $EL2$." This list has been constructed after Ref. 2 and completed with results of recent experimental studies.

(1) The normal or fundamental state of $EL2$ (labeled $EL2$-F in the following) has a deep donor level at midgap ($E_V+0.75$ eV).

(2) $EL2$-F is neutral, when it shows the characteristic absorption (see Fig. 1). Thus, the deep level is a $0/+$ transition.[39]

(3) $EL2$-F is an intrinsic deep defect, i.e., impurities do not control its characteristic optical properties.

(4) Similarities between the optical properties of $EL2$-F and the paramagnetic $\mathrm{As}_{\mathrm{Ga}}$ antisite[7,25-27,15-17] indicate that $EL2$-F contains at least one $\mathrm{As}_{\mathrm{Ga}}$ antisite.

(5) In the neutral charge state[39] $EL2$-F is not paramagnetic.

(6) $EL2$-F is a deep double donor: In addition, to the $0/+$ level there is a $+/2+$ level, at $E_V+0.54$ eV.[40,41]

(7) There is no further level of $EL2$-F in the upper part

of the band gap.[27,40]

(8) The neutral *EL*2-*F* exhibits an internal optical transition at $1.0 < \hbar\omega < 1.3$ eV (see the hump in the solid line in Fig. 1) which contributes to absorption, but only little to conductivity.[28]

(9) A zero-phonon line has been observed 0.14 eV below the main peak.[28-32]

(10) Investigations of the zero-phonon line under uniaxial stress[28-32] reveal tetrahedral symmetry of *EL*2. Nevertheless, on the basis of these experiments we would not yet rule out that the center may be *weakly* perturbed from T_d symmetry.[42]

(11) Below 140 K, *EL*2-*F* can be optically bleached by photons from the internal transition range (see Fig. 1). The bleached or metastable atomic configuration of *EL*2 will be labeled as *EL*2-*M*.

(12) *EL*2-*M* is electrically, optically and magnetically not active.

(13) The charge state of *EL*2-*M* is identical to that of *EL*2-*F* [see item (2) above].

(14) *EL*2-*F* can be thermally regenerated ($T > 140$ K). The barrier for thermal regeneration is 0.34 eV.

(15) The presence of electrons in the conduction band lowers the barrier to 0.1 eV (so-called electron-induced or Auger-like deexcitation).

(16) By high temperature [$T > 850$ °C (Ref. 13) or 1050 °C (Refs. 43 and 44)] *EL*2 can be destroyed.

(17) By annealing the sample at $T = 130$°C (Ref. 13) or 850° C (Refs. 43 and 44) *EL*2 is regenerated.

There are many more experimental data available which are more or less directly related to *EL*2. We have considered only those experimental results for this list, which refer to the neutral charge state,[39] and where experimental data *and* their analysis are confirmed by more then one group. We were forced to this approach, because many experimental papers in the literature seem to contradict others. In fact, even some points of our list may be questioned by some experimental analysis (as was noted in the list), but they are not in conflict with experimental data. We certainly do not want to disqualify those studied, which are not considered for the list, but for our needs the list is sufficiently long and covers a wide range of different properties, so that it can be used for detailed comparison with our later discussed theoretical results.

III. METHOD OF CALCULATION

We use density-functional theory[45] (DFT) together with the local-density approximation (LDA) for exchange and correlations.[46] The frozen-core approximation is applied and the frozen-core Ga^{3+} and As^{5+} ions are replaced by first-principles norm-conserving pseudopotentials.[47,48] The *s* and *p* nonlocality is treated exactly, but for *d* and higher spherical waves we use the same potential as for the *p* states. This saves computer time, but also affects the potential seen by *d* states close to the nuclei. We believe that this approximation is not severe, because the valence states of Ga and As are *s* and *p*, and close to the nucleus the potential for *d* and higher states is largely determined by the centrifugal potential $\hbar^2 l(l+1)/(2mr^2)$. Nevertheless, this approximation of the *d* potential results in errors of about 5% of the perfect GaAs lattice constant and about 15% for the bulk modulus compared to the experimental results.

We use a 54-atom fcc cell repeated periodically to build an infinite crystal. Viewed from a Ga-site defect, such a cell contains the four nearest neighbors (arsenic), the twelve second-nearest neighbors (gallium), the 12 third-nearest neighbors (arsenic), and the six fourth-nearest neighbors (gallium) completely; some atoms of the fifth-, sixth-, and seventh-nearest-neighbor shells are contained in the supercell as well. The electron density is calculated from the Γ point of the supercell Brillouin zone.

The Kohn-Sham equation,

$$h[n(\mathbf{r})]\Phi_i = \varepsilon_i \Phi_i \ , \tag{3.1}$$

with

$$h = -\frac{\hbar^2}{2m}\nabla^2 + V_{\mathrm{eff}}[n(\mathbf{r})] \ , \tag{3.2}$$

and

$$n(\mathbf{r}) = \sum_{\substack{\text{occupied}\\ \text{states}}} |\Phi_i|^2 \tag{3.3}$$

is solved using the method of Car and Parrinello.[49,50] Thus, a fictitious equation of motion for the occupied (and few unoccupied) Kohn-Sham eigenfunctions Φ_i is integrated numerically. The artificial evolution of these wave functions is given by

$$\mu \frac{\partial^2 \Phi_i}{\partial t^2} = \langle \Phi_i | h | \Phi_i \rangle \Phi_i - h\Phi_i \ . \tag{3.4}$$

This equation has to be solved under the constraint

$$\langle \Phi_i | \Phi_j \rangle = \delta_{ij} \tag{3.5}$$

for the orthonormality. Here, μ stands for a fictitious wave-function mass. The right-hand side of (3.4) expresses the fictitious force acting on the wave function Φ_i by the Hamiltonian $h[n(\mathbf{r})]$ and the reaction of the constraint. This force vanishes for all single-particle wave functions Φ_i if and only if these wave functions fulfill the Kohn-Sham equation (3.1) self-consistently. Thus, the result is identical to that of a standard self-consistent approach based on matrix-diagonalization methods. The advantage of the Car-Parrinello method is that the matrix diagonalization is performed iteratively only for the lowest (i.e., occupied) eigenvalues and wave functions, and simultaneously with the self-consistent update of the effective potential. A further advantage of the method, namely the simultaneous optimization of the atomic geometry, is not used in the present study, because it would have taken too much computer time (if we wanted to use a sufficiently complete basis). We therefore preferred to move the atoms "by hand," according to the self-consistently calculated forces.

The use of a supercell facilitates the calculations substantially if compared to Green-function methods. However, it also leads to an artificial defect band structure. Therefore the identification of defect-level positions is less accurate. Total energies and forces are affected only slightly by this problem, because the defect-induced perturbation is efficiently screened by the valence electrons and the charge-density change is very localized.

IV. RESULTS

A. The isolated arsenic antisite in its electronic ground state

Our calculations for the isolated $\mathrm{As_{Ga}}$ antisite show that this center is a deep double donor with its deep-level wave function belonging to the A_1 representation of the T_d point group. The wave function is displayed in Fig. 3, bottom. In the neutral charge state this a_1 level is filled with two electrons of opposite spin. The defect is therefore not paramagnetic when electrically neutral ($\mathrm{As_{Ga}^0}$) and when double positively charged ($\mathrm{As_{Ga}^{2+}}$). It is paramagnetic when single positively charged ($\mathrm{As_{Ga}^+}$). The first donor level is found at midgap. As can be seen in Fig. 3, its wave function is antibonding with respect to the central $\mathrm{As_{Ga}}$ atom and its four arsenic neighbors. The two electrons in the deep-level wave function of the neutral charge state therefore weaken the chemical bond: they effectively cancel one of the four $\mathrm{As_{Ga}}$—As bonds. About 1 eV above the midgap a_1 level the calculations predict an empty resonance state, which belongs to the t_2 representation of the T_d point group. Its wave function is shown at the top of Fig. 3. The t_2 state, like the a_1 state, has antibonding character. All these results are in good agreement with previous self-consistent Green-function calculations.[51,37,38]

When the nearest neighbors of the neutral antisite are allowed to relax, they move outwards by 4% of the perfect-crystal Ga-As bond length. The energy gained by this relaxation is 0.33 eV, which corresponds to a force constant $k_b = 52$ eV/Å^2. This force constant is similar to that of the other deep defects in semiconductors (e.g., chalcogens in silicon[52]). The moderate outwards breathing relaxation of the $\mathrm{As_{Ga}}$ antisite of about 4%, found in our calculations, may be compared with the 1% outward relaxation obtained by the Green-function calculations of Bachelet and Scheffler[37,38] and to the 8% obtained by Chadi and Chang.[53] We consider the differences with these two other calculations as minor, as they correspond to length differences of only 0.1 Å. They are probably due to the fact that Bachelet and Scheffler used local pseudopotentials, which also gave a higher breathing-mode force constant, and Chadi and Chang used a smaller super cell (18 atoms).

In agreement with earlier conclusions,[37,38] we find that *in the electronic ground state* the $\mathrm{As_{Ga}}$ antisite is a rather well-behaved defect, without giving a clear indication of an unstable or metastable behavior (see also the F total-energy curve in Fig. 4 for displacements <0.5 Å). With this respect as well as with respect to the electronic wave functions, the $\mathrm{As_{Ga}}$ antisite in GaAs is qualitatively identical to other substitutional deep double donors in semiconductors, such as, for example, chalcogens in silicon.[37,52]

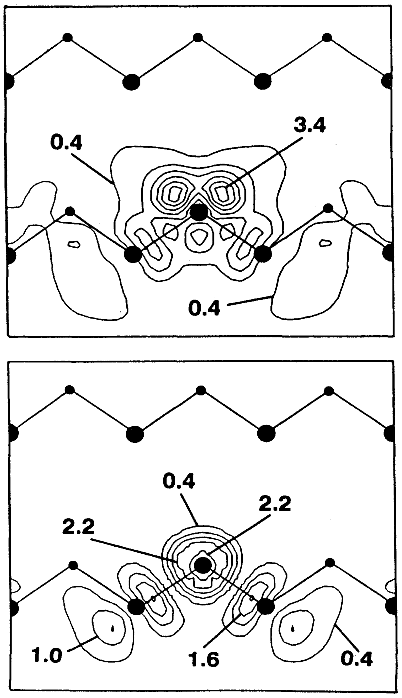

FIG. 3. Squared single-particle wave functions of the filled a_1 state (bottom) and the empty t_2 state (top) of the tetrahedral arsenic antisite. View on the (110) plane. Large circles are As nuclei, small circles are Ga nuclei. The contour lines are in units of electrons per bulk GaAs unit-cell volume.

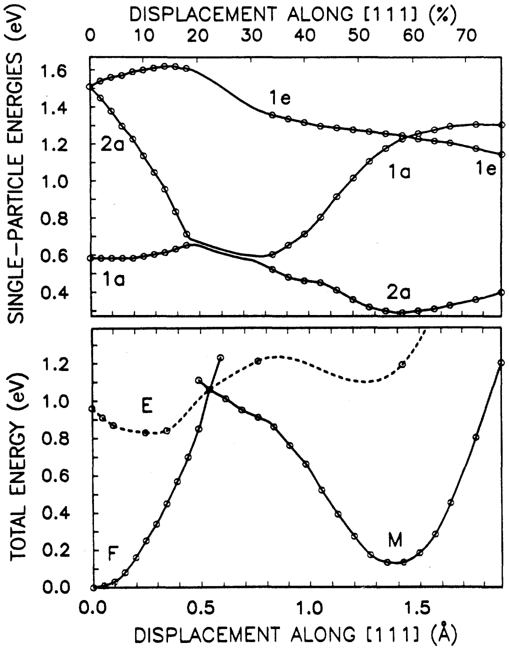

FIG. 4. Single-particle energies with respect to the valence-band edge (top), and total energies of the $S=0$ ground states (curves F and M) as functions of the position of the arsenic defect atom (bottom). Zero displacement refers to the tetrahedral As-antisite configuration. The total-energy curve labeled E is an electronic excited state with electronic configuration $1a^1 2a^1$. These calculations were performed with a basis set of $E_{\mathrm{cut}} = 8$ Ry, keeping all neighbors of the displaced arsenic atom at their perfect-crystal positions (see text).

B. Electronic excitation of the tetrahedral As antisite

Scheffler *et al.*[37] predicted that the excited electronic configuration $a_1^1t_2^1$ of tetrahedral, substitutional double donors can induce lattice distortions, which could be the origin of the photoquenching observed for some deep donors. The many-electron wave functions of this electronic configuration are a $^1T_2$ and a $^3T_2$ state. These two excited states are orthogonal to the $a_1^2t_2^0$ ground state and, therefore, they are, in fact, both ground states of T_2 symmetry and $S=0$ and $S=1$, respectively. Therefore they are both described by density-functional theory. Optical excitation from the $S=0$ ground state will end in the $^1T_2$ state. A spin-restricted theory gives an average energy of the $^1T_2$ and $^3T_2$ states. From the localization of the a_1 and t_2 wave functions we estimate that the $S=1$ state ($^3T_2$) has about 0.1 eV lower energy than the $S=0$ state ($^1T_2$). Because this splitting is small, we will not distinguish between these states in our calculations and continue to use a spin-restricted theory. The energy to excite one of the a_1 electrons of the neutral antisite to the t_2 resonant state (compare Fig. 3) is calculated as 0.97 eV before lattice relaxation. This energy thus corresponds to the Franck-Condon transition. We also note that the probability of an optical excitation is expected to be large for this $a_1 \rightarrow t_2$ transition, because both wave functions are well localized in the same region of space (see Fig. 3).

Both the $S=1$ and $S=0$ $a_1^1t_2^1$ excited states are orbital degenerate. As a consequence, the system is unstable with respect to a symmetry lowering Jahn-Teller distortion. We investigated distortions where the central arsenic defect atom is displaced in the [100], [110], and [111] directions. The Jahn-Teller force for the [111] displacement was found to be about twice as large as those for the other displacements. Thus we expect that the Jahn-Teller effect will move the central atom in the [111] direction towards the nearest T_d interstitial site. This lowers the symmetry of the defect to C_{3v} and results in a splitting of the t_2 state (top of Fig. 3) into a lower *a* state and higher *e* state. Only the *a* state is occupied with one electron, which is the reason for the Jahn-Teller energy gain. In the C_{3v} point group the electronic configuration of the excited state is now labeled as $1a^12a^1$. The C_{3v} $1a$ state corresponds to the T_d a_1 state of Fig. 3(a), and the C_{3v} $2a$ state is one component of the threefold degenerate t_2 state [Fig. 3(b)].

C. The transition to the metastable configuration

From now on we use the notation of the C_{3v} point group. Then, the many-electron wave functions of the excited configuration discussed in Sec. III B, are labeled ^1A and ^3A. The ^3A ($1a^12a^1$) state is the *ground state* for $S=1$, and the ^1A ($1a^12a^1$) state is an *excited state* for $S=0$, because it has the same symmetry as the ^1A ($1a^22a^0$) ground state. Density-functional theory can correctly describe the ^3A ($1a^12a^1$) state, but not the ^1A ($1a^12a^1$) state. A spin-restricted calculation gives some average energy of these two many-electron states. From the localization of the wave functions, we estimated that the splitting between both states is between 0.1 and 0.3 eV for all distortions considered in this paper. We therefore continue to use a spin-restricted calculation.

We showed that when the tetrahedral, neutral arsenic antisite is excited to the ^1A ($1a^12a^1$) and ^3A ($1a^12a^1$) states, Jahn-Teller forces will move the central arsenic defect atom in the [111] direction. Figure 4 displays the single-particle energies of the $1a$, $2a$, and $1e$ states (top), as well as the three total-energy curves obtained for the three electronic configurations $1a^22a^0$ (labeled *F*, which stands for fundamental), $1a^12a^1$ (labeled *E*, which stands for excited), and $1a^02a^2$ (labeled *M*, which stands for metastable). This figure should be taken in a semiquantitative way. It shows results of parameter-free calculations, but we applied two constraints: only one atom is moved, and all others are kept at their perfect-crystal positions. Furthermore, we used a smaller basis set ($E_{\text{cut}}=8$ Ry). Removing the two constraints will lower the total energies, but it will not change the general picture. In fact, we are unable to evaluate the total-energy curve on a mesh as dense as that of Fig. 4 without these constraints. Therefore, at first, we discuss the results shown in Fig. 4, and only at the end of subsection D do we consider the quantitative modifications which arise when the basis set is increased and when all atoms are allowed to relax.

As discussed in the preceding subsection, the Jahn-Teller theorem predicts that the *E* total-energy curve decreases, if the symmetry is reduce from T_d, i.e., if the As_{Ga} atom is displaced from its central position. In the neighborhood of the T_d configuration this energy gain can be also estimated from the slope of the single-particle level $2a$, shown in Fig. 4, top. The Jahn-Teller effect only starts the distortion. Already after a small displacement we find that the different wave functions (namely the $1a$ and $2a$ single-particle states) start to mix. In Fig. 4 we find a minimum of the *E* total-energy curve for the 0.3-Å displaced arsenic defect. This geometry may play a role in a non-Franck-Condon excitation and we therefore expect a zero-phonon line at about 0.1–0.2 eV below the main peak.

It is most likely that the excited system falls back down to the *F* curve, the ground-state total energy. Then the system ends up again as a tetrahedral As_{Ga} antisite. However, Fig. 4 shows that the $2a$ single-electron level decreases in energy very rapidly and therefore starts to mix with the $1a$ state. This allows for another electronic configuration, namely $1a^02a^2$. Thus, once excited to the *E* curve, the system has a certain probability of changing to the *M* curve. Then the arsenic defect atom will end up considerably far away (about 1.4 Å) from its initial, central gallium site. We refer to this metastable atomic configuration as the gallium-vacancy–arsenic-interstitial pair. The As interstitial is about 1 Å away from the T_d interstitial site. It is therefore chemically bound to only three arsenic atoms.[54] The transition to the metastable state competes with two other possible processes, namely the ionization of the excited state (where the excited electron of the As_{Ga} goes to the conduction band) and the deexcitation ($1a^12a^1 \rightarrow 1a^22a^0$) at smaller distortions. These two processes will bring the arsenic defect atom back to the fundamental configuration, i.e., the tetrahedral $\mathrm{As}_{\mathrm{Ga}}$ antisite. Because of these competitors, it is obvious that the probability of the metastable transition is small and that it should be sensitive to local stress and other perturbations. It also depends sensitively on the conduction-band structure.

As the arsenic defect atom leaves the gallium site, its bond with one arsenic neighbor that is left behind is stretched and it almost breaks when the defect enters the barrier region. This is shown in Fig. 5. The barrier of the structural transition is reached when the arsenic atom passes through the (111) plane of three As neighbors (see Fig. 6). In the metastable configuration the arsenic defect atom (now an interstitial) binds to these three atoms (see Figs. 5 and 6), similar to the bonding in crystalline grey arsenic. In the vacancy region there is one broken bond, which is filled with two electrons.

The electronic structure of the vacancy-interstitial pair found in our self-consistent calculations (top of Fig. 4 at 1.4 Å displacement) can be summarized qualitatively in terms of a simple tight-binding picture. The left- and right-hand parts of Fig. 7 show schematically the electronic structure of the isolated gallium vacancy and of an isolated arsenic interstitial. The vacancy (T_d symmetry) has a t_2 state close to the valence-band edge; in the neutral charge state this level (which can hold up to six electrons) is filled with three electrons. Furthermore, the vacancy has an a_1-resonant state in the valence band. The arsenic interstitial at a C_{3v} symmetry site has an a level in the lower and an e level in the upper half of the band gap. In the neutral interstitial, the a state is filled with two electrons and the e state is filled with one electron. When the two systems interact (the middle part of Fig. 7), the e component of the vacancy t_2 level and the interstitial e state form a bonding and an antibonding level, which both disappear from the gap. The interaction of the two vacancy a with the interstitial a states is slightly more complicated, but also follows qualitatively the tight-binding picture (see Fig. 7). The five electrons of the neutral gallium vacancy and the three electrons of the neutral arsenic interstitial will fill the three energetically lowest levels of the pair. From the wave-function character of the occupied states we may label the pair $V_{\mathrm{Ga}}^{-}\mathrm{As}_i^{+}$. Our self-consistent calculations give that the empty a and

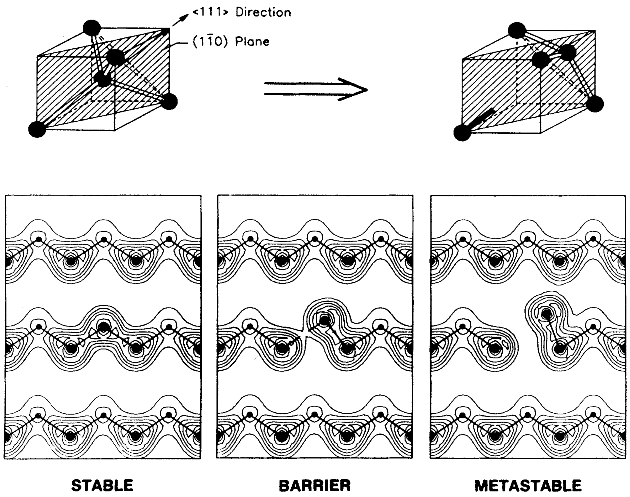

FIG. 5. Metastability of the As-antisite defect. Top: atomic structure. Bottom: the electron density in the (110) plane. Large circles represent As nuclei. Small circles represent Ga nuclei. The left-hand side shows the fundamental state, where the arsenic defect atom is bound to four nearest neighbors [only two are in the displayed (110) plane]. The middle panel shows the barrier region. The picture on the right-hand side corresponds to the metastable situation (the $V_{\mathrm{Ga}}\mathrm{As}_i$ defect pair). Here the arsenic defect is bound to three arsenic neighbors [only one of them is in the (110) plane]. The solid "dangling bond" in the top right-hand picture indicates the vacancy state (also see the bottom of Fig. 8), which is responsible for the barrier between the metastable and the fundamental configuration.

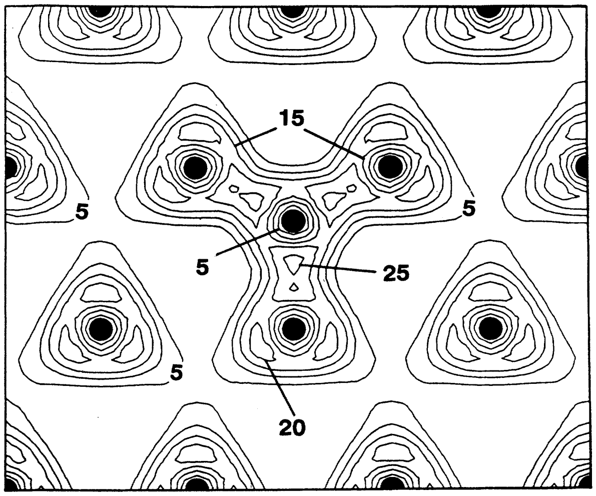

FIG. 6. Total valence-electron density in the atomic configuration of the barrier. View on the (111) plane (the triangle marked by a dashed line in Fig. 5). The counter lines are in units of electrons per bulk GaAs unit-cell volume.

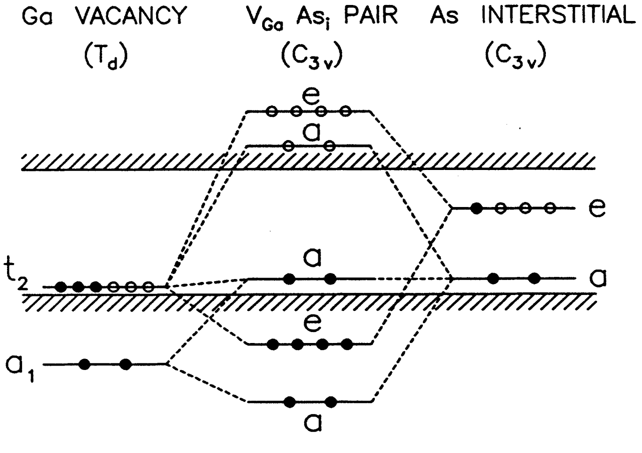

FIG. 7. Schematic summary of the electronic structure of the metastable configuration, i.e., of the $V_{\mathrm{Ga}}^{-}\mathrm{As}_i^{+}$ defect pair (middle), which can be understood in terms of a Ga vacancy (left) interacting with a C_{3v}-site As-interstitial (right).

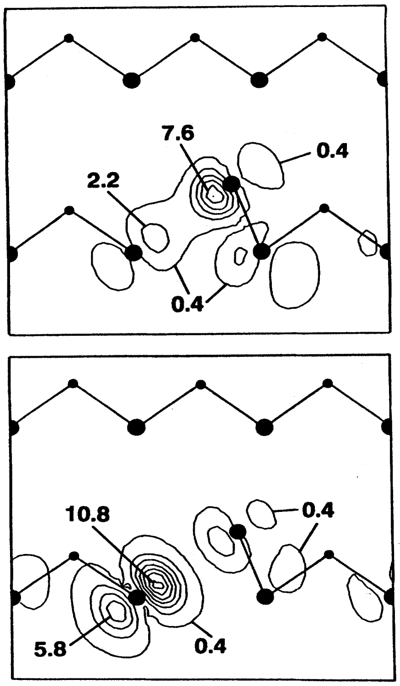

FIG. 8. Squared single-particle wave functions of the filled $2a$ (bottom) and the empty $1a$ state (top) of the metastable configuration (compare Fig. 4 at a displacement of 1.4 Å). View on the (110) plane. Small circles represent Ga nuclei, large circles are As nuclei. The contour lines are in units of electrons per bulk GaAs unit-cell volume.

e states of the pair are close to the conduction-band edge. The highest filled state (labeled $2a$ in Fig. 4) is close to the valence-band edge; it has vacancy dangling-bond character, as can be seen in Fig. 8. This wave function is very localized. Our calculations give its eigenvalue at about 0.3 eV above the valence-band edge. The corresponding $(0/+)$ electronic level would then be degenerate with the valence-band top. The $(-/0)$ electronic level of the metastable configuration is found close to the conduction-band edge. We therefore expect that the gallium-vacancy—arsenic-interstitial pair configuration is electrically not active. The energy for an internal optical excitation ($2a \rightarrow e$ in Fig. 4) may be below the width of the band gap. However, the initial state ($2a$, vacancylike) and final state (e interstitial-like) are spatially separated (see Fig. 8) and the corresponding optical cross section should be small.

D. The barrier of the neutral charge state

Our constrained calculations shown in Fig. 4 give a barrier for the neutral ground state of 0.92 eV between the minimum of the metastable configuration (the $V_{\mathrm{Ga}}\mathrm{As}_i$ pair) and the fundamental configuration (the $\mathrm{As}_{\mathrm{Ga}}$ antisite). This value decreases if the two constraints are relaxed, i.e., if we increase the basis set and if we allow the atoms of the cell to relax. We performed calculations using a large basis set ($E_{\mathrm{cut}}=20$ Ry) for the two minima and the maximum of the total-energy configuration of Fig. 2. From the calculated forces and force constants, we estimated the lattice relaxation. Furthermore, we estimated the effect of spin polarization, which is particularly large at the barrier configuration, where the wave functions are very localized. We then obtain a barrier of about 0.4 eV.

Figure 4 shows that the fourfold-coordinated $\mathrm{As}_{\mathrm{Ga}}$ antisite and the metastable configuration with the threefold-coordinated As_i have very similar total energy. On the basis of the arguments presented, this result is indeed plausible for a group-V element. The origin of the barrier between the two configurations is, however, not obvious. It may be understood by the fact that the covalent radius of an As atom is 1.2 Å. Therefore the As_i is too "thick" to pass easily through the (111) plane of the three As atoms. This argument is, however, not complete and cannot explain why for other charge states the barrier will in fact disappear (see the next subsection below). The main reason for the barrier is the filled vacancylike dangling bond shown in Figs. 5 and 8. This state is antibonding with respect to the arsenic interstitial, and its energy (the $2a$ level in Fig. 4) increases if the As interstitial is moved from the metastable configuration towards the vacancy. The occupied vacancy dangling orbital therefore contributes to the repulsion between the constituents of the metastable pair. It is obvious that the barrier will change if one electron is removed from this level.

E. The barrier of the single positive and single negative charge states

The ground-state total energy for the positive charged center is given by

$$E^{+}=E^{0}-\varepsilon(+/0)+E_F \ . \tag{3.6}$$

E^0 is the neutral-charge-state total energy, i.e., the F and M curves of Fig. 4, $\varepsilon(+/0)$ is the transition state[55] of the highest occupied single-particle level (see Fig. 4), and E_F is the Fermi level, to which the electron is transferred. We obtain that the barrier is significantly reduced for the E^+ total energy, compared to E^0, namely by 0.4 eV. Thus, the barrier practically vanishes when we remove one electron from the vacancylike dangling orbital of the $V_{\mathrm{Ga}}\mathrm{As}_i$ pair, shown in Figs. 5 and 8. This implies that a positive-charged $\mathrm{As}_{\mathrm{Ga}}$ should not exhibit metastable behavior.

This result suggests that a transition from the metastable to stable configuration can be induced by (a temporary) hole capture at the $V_{\mathrm{Ga}}\mathrm{As}_i$. This is, *in principle*, possible. The probability of this effect scales with the lifetime of the hole in the $2a$ level of the $V_{\mathrm{Ga}}\mathrm{As}_i$. This is analogous to the $\mathrm{As}_{\mathrm{Ga}} \rightarrow V_{\mathrm{Ga}}\mathrm{As}_i$ transition which scales with the lifetime of the excited electron in the $2a$ level at the $\mathrm{As}_{\mathrm{Ga}}$. The lifetime has to be compared with the time scale of the atomic rearrangement. The lifetime of the excited $\mathrm{As}_{\mathrm{Ga}}$ electron is high, because this electron is in an energy region of the conduction band with a very low density of states. On the other hand, the hole in the $V_{\mathrm{Ga}}\mathrm{As}_i$ $2a$ state has an energy at the valence-band top, where the density of states is high. We therefore expect that the probability of a hole-induced regeneration should be small.

A second possibility of the $V_{\mathrm{Ga}}\mathrm{As}_i \rightarrow \mathrm{As}_{\mathrm{Ga}}$ regeneration is that an electron is (temporary) captured in the $1a$ level of the metastable system. This corresponds to a temporary negative charge state of the $V_{\mathrm{Ga}}\mathrm{As}_i$ pair. The total energy is given by

$$E^{-}=E^{0}+\varepsilon(0/-)-E_F \ . \qquad (3.7)$$

The transition-state energy $\varepsilon(0/-)$ corresponds to the $1a$ state of the metastable configuration in Fig. 4. Our calculations predict that the E^{-} total-energy curve is very flat. Thus, the barrier is close to zero, but there are no strong forces pulling the As_i to the vacancy. Still, because the density of states at the bottom of the GaAs conduction band is very small, the negative charge state may live sufficiently long. Thus, this electron-induced regeneration is a likely regeneration channel.

V. COMPARISON OF THE THEORETICAL RESULTS OF THE $\mathrm{As}_{\mathrm{Ga}} \leftrightarrows V_{\mathrm{Ga}}\mathrm{As}_i$ PROCESS TO THE $EL2$ PROPERTIES

The comparison of the above results for the isolated arsenic antisite and the $\mathrm{As}_{\mathrm{Ga}} \leftrightarrows V_{\mathrm{Ga}}\mathrm{As}_i$ metastability to the list of $EL2$-defect properties given in the Sec. II reveals clear similarities. Both defects have basically the same electronic structure: they are double donors and give rise to two deep levels. Both defects are not paramagnetic when in the charge state, which shows the midgap level and exhibits the metastability, and both do not have a level in the upper part of the gap. The internal excitation of both centers is practically identical; the theoretical value of the Franck-Condon transitions at an $\mathrm{As}_{\mathrm{Ga}}$ of 0.97 eV agrees well (within the expected accuracy of a parameter-free DFT-LDA calculation) with the $EL2$ absorption main peak at 1.18 eV. The zero-phonon line in the experiments (0.14 eV below the main peak) may be compared to the theoretical result of 0.13 eV. However, here it is not yet clear if the experimental zero-phonon line is indeed a transition to the [111]-displaced arsenic defect atom.

We found that optical excitation of the $\mathrm{As}_{\mathrm{Ga}}$ can induce a structural transition via the intermediate total-energy curve labeled E in Fig. 4. The mechanism implies that the probability of this bleaching effect should be sensitive to the quality of the crystal. This is indeed known experimentally, where no bleaching was observed in strongly perturbed samples. For the positive charge state of the $\mathrm{As}_{\mathrm{Ga}}$ antisite, in particular, theory and experiment tell that this is not quenchable directly, but only after the $\mathrm{As}_{\mathrm{Ga}}^{+}$ is transformed to an $\mathrm{As}_{\mathrm{Ga}}^{0}$. The theoretical barrier height for thermal recovery (i.e., for the $V_{\mathrm{Ga}}\mathrm{As} \rightarrow \mathrm{As}_{\mathrm{Ga}}$ transition) of 0.4 eV is close to the experimental value of 0.34 eV. This good agreement may be fortuitous, because the calculated barrier height is sensitive to the lattice relaxation. Also, the regeneration conditions are the same in our calculations and in experiments of $EL2$: there is the purely thermal process and an electron-induced ("Auger-like") regeneration process. The electron-induced deexcitation of $EL2$ can be understood in our above-discussed theory in the following way: It starts with a thermally activated capture of a conduction-band electron in the $1a$ resonant state of the $V_{\mathrm{Ga}}\mathrm{As}_i$ pair. This capture is then followed by relaxation of the As_i to the fundamental configuration, where the captured electron is released. The third channel of regeneration of the fundamental atomic configuration, namely the hole induced deexcitation, is expected to have a very small cross section. Indeed, such a process has not yet been observed for $EL2$.

Combined EPR-DLTS studies of von Bardeleben *et al.*[13] indicated that $EL2$ is destroyed if the sample is heated to 850 °C and rapidly cooled afterwards, but it can be regenerated by 130 °C annealing. This result can be qualitatively explained as follows: at high temperatures the $\mathrm{As}_{\mathrm{Ga}} \leftrightarrows V_{\mathrm{Ga}}\mathrm{As}_i$ system dissociates into a gallium vacancy and an arsenic interstitial. Rapid cooling hinders the reverse process and additional annealing at intermediate temperatures would be necessary to allow for the diffusion of the As_i and the association reaction $V_{\mathrm{Ga}}+\mathrm{As}_i \rightarrow \mathrm{As}_{\mathrm{Ga}}$. Again, as in many $EL2$-related experiments, the results of Ref. 13 have not been fully reproduced by other researchers. Lagowski *et al.*[43,44] report different temperatures, namely 1050 °C (instead of 850 °C) and 850 °C (instead of 130 °C). This demonstrates the high complexity of $EL2$ investigations: experimental results seem to depend strongly on the sample and on the crystal environment. For a more general discussion of how the crystal Fermi level (i.e., the electron chemical potential) and the gas in the crystal environment (the atomic chemical potential) can influence defect reactions and formation energies we refer to our paper.[56]

As stated in the Introduction, several experiments[15–17,34–57] and theoretical studies[18–21] indicated that $EL2$ is an axial defect, namely the distant $\mathrm{As}_{\mathrm{Ga}}$-$\mathrm{As}_i$ defect pair. The charge state of $EL2$ was determined to be positive when it undergoes the metastable transition,[39] and the distance of the double positive center was deduced from ENDOR as 4.88 Å.[15–17] We cannot disprove these experimental interpretations, but we note that they are in conflict with others. We now discuss these experimental results which could rule against the identification of $EL2$ with the arsenic antisite, and we will argue that the experimental data are, in fact, not necessarily at variance with the proposal that the $\mathrm{As}_{\mathrm{Ga}}$ antisite actuates the metastability.

DLTS investigations of the metastable transition of $EL2$ under stress[34] were interpreted such that the fundamental state of $EL2$ has C_{3v} symmetry; this would rule against the isolated $\mathrm{As}_{\mathrm{Ga}}$. However, at present we consider the absorption measurements[28–32] as the more direct study of the symmetry of the fundamental state of $EL2$, and these experiments show that the defect symmetry is T_d. We suggest that the data of Ref. 34 can be also interpreted such that the metastability transition goes from a T_d- to a C_{3v}-symmetry configuration. According to our calculations, the metastable transition is sensitive to the positions of the nearest neighbors of the antisite, because on its way to the metastable site the defect has to pass between three of these atoms (see Fig. 5). By uniaxial stress the probabilities of the transitions in the four different [111] directions become different. The actual direction of the displacement of the arsenic defect atom is determined by the orientation of the excited electron's orbital and this can be controlled by the polarization of the optical excitation. The observed[34] dichromatic behavior of the $EL2$ transition rate may be due to this effect.

As a second example of experiments interpreted in terms of an $EL2$ axial character, we discuss the ENDOR studies of Meyer *et al.*[15–17] We emphasize that these experiments measure a charge state different from that which we are interested in here: $EL2$ is not paramagnetic, when it is in the charge state which shows the metastable transition. Nevertheless, Meyer *et al.* claimed that the structure of their center is identical with $EL2$. On the other hand, we noted[3,22–24] that in an annealed sample a neutral and a positive $\mathrm{As_{Ga}}$ antisite can have a different local environment (also see the discussion of the iron-acceptor pairs in Ref. 3). This is experimentally indicated by the fact that $EL2^0$ and $EL2^+$ show an anticorrelated distribution over a wafer, which means that $EL2^0$ and $EL2^+$ are found in different regions of the sample. Thus, $EL2^+$ may be a complex ($\mathrm{As_{Ga}}$ together with an acceptor), which makes the $\mathrm{As_{Ga}}$ component paramagnetic and observable by magnetic circular dichroism (MCD) and ENDOR, but $\mathrm{EL2^0}$ may be the "simple" center.

Another effect, which may obscure the interpretation of experimental data obtained on semi-insulating samples, is the change of Fermi energy due to the metastable transition of $EL2$. In a semi-insulating crystal the Fermi level is pinned to the midgap level of $EL2$. Therefore a significant number (of order 10^{16} $\mathrm{cm^{-3}}$) of positively charged $EL2$ centers must exist. As noted above, these centers cannot be bleached directly, but must be first neutralized with electrons. The need to bring 10^{16} electrons from other defects, and the fact that they will come back to these defects only after regeneration of the fundamental state of $EL2$, may induce *indirect* effects of the $EL2$ metastability. For instance, the anisotropic change observed in ballistic-phonon scattering after the bleaching of $EL2$ (Ref. 57) may be due to a change of the $EL2$ phonon-scattering cross section or to changes of other defects caused by the change of their charge states.

The above discussion shows that the identification of $EL2$ with the arsenic antisite is, in fact, not at variance with those experimental data interpreted as favoring an axial defect. From the similarities between the theoretical results of Sec. IV and the various $EL2$ properties listed in Sec. II, we therefore identify the mechanism of the $EL2$ metastability as that of the $\mathrm{As_{Ga}} \leftrightarrows V_{\mathrm{Ga}}\mathrm{As}_i$ process. This makes a complex unlikely, but it does not necessarily rule out a weakly interacting $\mathrm{As_{Ga}}$-X center, where the $\mathrm{As_{Ga}}$ component is neutral. The interaction between the unknown X and $\mathrm{As_{Ga}}$ should be, however, very weak, so that the identified mechanism of the optically inducible structural transition is not destroyed.

VI. CONCLUSIONS

The above-described calculations show that the neutral arsenic antisite exhibits, under optical excitation, an intrinsic metastability. In the metastable atomic configuration, which corresponds to a close gallium-vacancy–arsenic-interstitial pair, the surplus arsenic atom builds up a threefold bonding. This $\mathrm{As_{Ga}} \leftrightarrows V_{\mathrm{Ga}}\mathrm{As}_i$ process was only recently found to be a likely reaction. The metastable transition is started by a Jahn-Teller effect, as speculated already in Ref. 37 and 38. We noted that the $\mathrm{As_{Ga}} \leftrightarrows V_{\mathrm{Ga}}\mathrm{As}_i$ system exhibits essentially the same behavior as that known for the famous $EL2$ center, and we considered 17 of the most characteristic properties of $EL2$. In particular, the good agreement between the calculated barrier (0.4 eV) and the experimental barrier suggests that the $\mathrm{As_{Ga}}$ antisite and $EL2$ are identical defects. The uncertainty in our calculations is estimated as ± 0.2 eV. Therefore we cannot rule out for sure that another nearby (but weakly interacting) defect is in fact necessary to adjust the barrier at the 0.34 eV observed for $EL2$. Nevertheless, based on a detailed comparison with many experimental properties, we identified the basic mechanism of the $EL2$ metastability as that of the $\mathrm{As_{Ga}}$ antisite.

We also noted that this new type of metastability should be common to many substitutional defects in semiconductors—it resembles properties of the diamond $\leftrightarrows$ graphite metastability. We cannot predict, however, without a full calculation, for which defects this mechanism will be observable: The height of the barrier and the energy difference between the fundamental and metastable configurations will be different for different systems. A system very similar to the neutral $\mathrm{As_{Ga}}$ antisite is the negatively charged substitutional silicon, $\mathrm{Si_{Ga}}$, in GaAs. The bonding character and number of electrons are the same. Indeed, according to calculations of Chadi and Chang,[58] this defect shows a $\mathrm{Si_{Ga}} \leftrightarrows V_{\mathrm{Ga}}\mathrm{Si}_i$ metastable behavior. The properties of the $\mathrm{Si_{Ga}}$ or $V_{\mathrm{Ga}}\mathrm{Si}_i$ defect seem to explain the properties of the famous DX centers in $\mathrm{Ga}_{1-x}\mathrm{Al}_x\mathrm{As}$ and in GaAs under pressure. We would also like to mention a somewhat similar phenomenon in group-IVA elements (e.g., Ti and Zr), which are the transition-metals counterparts of the group-IVB elements (e.g., C or Si). Group-IVA elements show a phase transition from the bcc to the hexagonal structure, the so-called ω phase, in which the atoms are trigonally bonded. In the bcc phase a so-called ω embryo can be formed, which explains certain self-diffusion properties in these materials.[59,60] Analogously, we feel that the $\mathrm{As_{Ga}} \leftrightarrows V_{\mathrm{Ga}}\mathrm{As}_i$ type of process may be also important for defect diffusion in semiconductors (see, for example, Ref. 61).

ACKNOWLEDGMENTS

We are grateful to Gene Baraff, Tadeusz Figielski, Rainer Gillert, Martina Heinemann, Wojtek Kuszko, Tom Morgan, Eicke Weber, and Tadeusz Wosinski for stimulating and helpful discussions. We thank Roberto Car and Michelle Parrinello for making their computer code available for us. One of us (J.D.) wants to thank the Deutscher Akademischer Austauschdienst for financial support. Part of this work was supported by the Stiftung Volkswagenwerk (West Germany) and by Project No. CPBP 01.05 of the Warsaw University.

*Present address: Instytut Fizyki Polskiej Akademii Nauk, Aleja Lotników 32, 02-668 Warszawa, Poland.

[1] G. M. Martin, Appl. Phys. Lett. **39**, 747 (1981).

[2] G. M. Martin and S. Makram-Ebeid, in *Deep Centers in Semiconductors,* edited by S. T. Pantelides (Gordon and Breach, New York, 1986), p. 231.

[3] M. Scheffler, in *Festköperprobleme XXIX (Advances in Solid State Physics),* edited by U. Rössler (Vieweg, Braunschweig, 1989), p. 231.

[4] G. D. Watkins, Mater. Sci. Form **38-41**, 39 (1989).

[5] A. Chantre and D. Bois, Phys. Rev. B **31**, 7979 (1985).

[6] J. J. van Kooten, G. A. Weller, and C. A. J. Ammerlaan, Phys. Rev. B **30**, 4564 (1984).

[7] E. R. Weber and P. Omling, in *Festkörperprobleme XXV (Advances in Solid State Physics),* edited by P. Grosse (Vieweg, Braunschweig, 1985), p. 623.

[8] W. Frank, in *Proceedings of the 12th Internationl Symposium on GaAs and Related Compounds,* edited by M. Fujimoto (Hilger, Bristol, 1986), p. 217.

[9] T. Figielski and T. Wosinski, Phys. Rev. B **36**, 1269 (1987).

[10] J. F. Wager and J. A. Van Vechten, Phys. Rev. B **35**, 1269 (1987).

[11] G. A. Baraff and M. Schlüter, Phys. Rev. Lett. **55**, 2340 (1985).

[12] H. J. von Bardeleben, D. Stievenard, J. C. Bourgoin, and A. Huber, Appl. Phys. Lett. **47**, 970 (1985).

[13] H. J. von Bardeleben, D. Stievenard, D. Deresmes, A. Huber, and J. C. Bourgoin, Phys. Rev. B **34**, 7192 (1986).

[14] J. C. Bourgoin, H. J. von Bardeleben, and D. Stievenard, J. Appl. Phys. **64**, R64 (1988).

[15] B. K. Meyer, D. M. Hofmann, and J.-M. Spaeth, Mater. Sci. Forum **10-12**, 311 (1986).

[16] B. K. Meyer, D. M. Hofmann, J. R. Niklas, and J.-M. Spaeth, Phys. Rev. B **36**, 1332 (1987).

[17] B. K. Meyer, Rev. Phys. Appl. **23**, 809 (1988).

[18] C. Delerue, M. Lannoo, and D. Stievenard, Phys. Rev. Lett. **59**, 2875 (1987).

[19] G. A. Baraff and M. Schlüter, Phys. Rev. B **35**, 6154 (1987).

[20] G. A. Baraff and M. Lannoo, Rev. Phys. Appl. **23**, 817 (1988).

[21] M. J. Caldas and A. Fazzio, Mater. Sci. Forum **38-41**, 119 (1989).

[22] J. Dabrowski and M. Scheffler, Phys. Rev. Lett. **60**, 2183 (1988).

[23] J. Dabrowski and M. Scheffler, in *Proceedings of the 5th Conference on Semi-insulating III-V Materials, Malmö, 1988,* edited by G. Grossmann and L. Ledebo (Hilger, Bristol, 1988), p. 37.

[24] J. Dabrowski and M. Scheffler, Mater. Sci. Forum **38-14**, 51 (1989).

[25] E. R. Weber, H. Ennen, U. Kaufmann, J. Windscheif, J. Schneider, and T. Wosinski, J. Appl. Phys. **53**, 6140 (1982).

[26] M. Wattenbach, J. Krüger, C. Kisielowski-Kemmerich, and H. Alexander, Mater. Sci. Forum **38-41**, 73 (1989).

[27] K. Elliott, R. T. Chen, S. G. Greenbaum, and R. J. Wagner, Appl. Phys. Lett. **44**, 907 (1984).

[28] M. Kaminska, M. Skowronski, and W. Kuszko, Phys. Rev. Lett. **55**, 2204 (1985).

[29] M. Kaminska, Phys. Scr. T **19**, 551 (1987).

[30] W. Kuszko, P. J. Walczak, P. Trautman, M. Kaminska, J. M. Baranowski, Mater. Sci. Forum **10-12**, 317 (1986).

[31] K. Bergman, P. Omling, L. Samuelson, and H. G. Grimmeiss, in *Proceedings of the 5th Conference on Semi-insulating III-V Materials, Malmö, 1988,* edited by G. Grossman and L. Ledebo (Hilger, Bristol, 1988), p. 397.

[32] R. Trautman, J. P. Walczak, and J. M. Baranowski (unpublished).

[33] T. Mochizuki and T. Ikoma, Phys. Rev. Lett. **59**, 590 (1987).

[34] M. Levinson and J. A. Kafalas, Phys. Rev. B **35**, 9383 (1987).

[35] G. A. Baraff, M. Lannoo, and M. Schlüter, in *Defects in Electronic Materials,* Mater. Res. Soc. Symp. Proc. No. 104, edited by M. Stavola, S. J. Pearton, and G. Davies (MRS, Pittsburgh, 1988), p. 375.

[36] It is well known, however, that localized defects couple to the *total* crystal phonon band structure [see, for example, the discussion of Fig. V, 52 in the article by U. Scherz, in *Lehrbuch der Experimentalphysik, Bergmann-Schaefer* (de Gruyter, Berlin, 1980), Vol. IV, p. 454]. If this is taken into account, the (average) Huang-Rhys factor is about 6, and then the theoretical line shape is not in conflict with the $EL2$ absorption.

[37] M. Scheffler, F. Beeler, O. Jepsen, O. Gunnarsson, O. K. Anderesen, and G. B. Bachelet, in *Proceedings of the 13th International Conference on Defects in Semiconductors,* edited by L. C. Kimerling and J. M. Parsey, Jr. (The Metallurgical Society of AIME, New York, 1984), p. 45.

[38] G. B. Bachelet and M. Scheffler, in *Proceedings of the 17th International Conference on the Physics of Semicondutors,* edited by J. D. Chadi and W. A. Harrison (Springer, New York, 1985), p. 755.

[39] The fact that the midgap level of $EL2$ is a $(0/+)$ transition is generally accepted, although no *direct* experimental measurement of the charge state exists. The indirect conclusion about the charge state is based on the role of $EL2$ in the compensation of "undoped" GaAs, i.e., on the fact that $EL2$ pins the Fermi level to the midgap position. Recently, it was suggested [H. J. von Bardeleben, D. Stievenard, H. R. Zelsmann, and J. C. Bougouin, in *Proceedings of the 5th Conference on Semi-insulating III-V Materials, Malmö, 1988,* edited by G. Grossmann and L. Ledebo (Hilger, Bristol, 1988), p. 127] that $EL2$ corresponds to a $(+/2+)$ transition. We feel that the question on the correct charge state is not yet unambiguosly settled. Following common practice, we call the charge state of $EL2$-F, which shows the characteristic absorption and the metastability, the neutral one.

[40] H. C. Gatos, and J. Lagowski, in *Microscopic Identification of Electronic Defects in Semiconductors,* Mater. Res. Soc. Symp. Proc. No. 46, edited by N. M. Johnson, S. G. Bishop, and G. D. Watkins (MRS Pittsburgh, 1985), p. 153.

[41] J. Osaka, H. Okamoto, and K. Kobayashi, in *Semi-Insulating III-V Materials,* edited by H. Kukimoto and S. Miyazawa (Omsha, Tokyo, 1986), p. 421.

[42] Recent investigations of M. Baj and P. Dreszer [Mater. Sci. Form **38-41**, 101 (1989)] show that under hydrostatic pressure the zero-phonon line and the main peak of the $EL2$ absorption move in different directions, thus suggesting that they are due to different transitions. This suggestion is, however, not yet conclusive, because the direct transition and the zero-phonon-line transition correspond to different atomic geometries of different symmetries and different electronic wave functions. Therefore, the reaction to hydrostatic pressure can be different. More theoretical work is necessary to understand these experiments.

[43] J. Lagowski, H. C. Gatos, C. H. Kang, M. Skowronski, K. Y. Ko, and D. G. Lin, Appl. Phys. Lett. **49**, 892 (1986).

[44] J. Lagowski (private communication).

[45] *The Inhomogeneous Electron Gas,* edited by N. H. March and S. Lundqvist (Plenum, New York, 1984).

[46] D. M. Ceperley and B. J. Alder, Phys. Rev. Lett. **45**, 566

(1980).

[47] D. R. Hamann, M. Schlüter, and C. Chiang, Phys. Rev. Lett. **43**, 1494 (1979).

[48] G. B. Bachelet, D. R. Hamann, and M. Schlüter, Phys. Rev. B **26**, 4199 (1982).

[49] R. Car and M. Parrinello, Phys. Rev. Lett. **55**, 2471 (1985).

[50] M. C. Payne, J. D. Joannopoulos, D. C. Allan, M. T. Teter, and D. H. Vanderbilt, Phys. Rev. Lett. **56**, 2656 (1986).

[51] G. B. Bachelet, M. Schlüter, and G. A. Baraff, Phys. Rev. B **27**, 2545 (1983).

[52] M. Scheffler, Physica B+C **146B**, 176 (1987).

[53] D. J. Chadi and K. J. Chang, Phys. Rev. Lett. **60**, 2187 (1988).

[54] The metastable configuration found in Fig. 4 is qualitatively and quantitatively different than that described in Ref. 30, because an As_i at the T_d interstitial site would be fourfold coordinated and would have a much higher energy.

[55] J. Janak, Phys. Rev. B **18**, 7165 (1978).

[56] M. Scheffler and J. Dabrowski, Philos. Mag. A **58**, 107 (1988).

[57] J. C. Culbertson, U. Strom, and S. A. Wolf, Phys. Rev. B **36**, 2962 (1987).

[58] D. J. Chadi and Chang, Phys. Rev. Lett. **61**, 873 (1988).

[59] J. M. Sanchez and D. de Fontaine, Phys. Rev. Lett. **35**, 227 (1975).

[60] U. Köhler and C. Herzig, Philos. Mag. A **58**, 769 (1988).

[61] M. K. Sheinkman, Acta. Phys. Pol. **73**, 925 (1988).